

RSC Advances



This is an *Accepted Manuscript*, which has been through the Royal Society of Chemistry peer review process and has been accepted for publication.

Accepted Manuscripts are published online shortly after acceptance, before technical editing, formatting and proof reading. Using this free service, authors can make their results available to the community, in citable form, before we publish the edited article. This *Accepted Manuscript* will be replaced by the edited, formatted and paginated article as soon as this is available.

You can find more information about *Accepted Manuscripts* in the [Information for Authors](#).

Please note that technical editing may introduce minor changes to the text and/or graphics, which may alter content. The journal's standard [Terms & Conditions](#) and the [Ethical guidelines](#) still apply. In no event shall the Royal Society of Chemistry be held responsible for any errors or omissions in this *Accepted Manuscript* or any consequences arising from the use of any information it contains.



COMMUNICATION

“Reactive nanoprecipitation”: a one-step route to functionalized polylactide-based nanoparticles

Received 00th January 20xx,
Accepted 00th January 20xx

Damien Ficheux,^a Céline Terrat,^a Bernard Verrier,^a Didier Gignes^b and Thomas Trimaille*^b

DOI: 10.1039/x0xx00000x

www.rsc.org/

We report here a straightforward nanoprecipitation-based process to prepare functionalized polylactide (PLA) nanoparticles (NPs). It relies on an organic phase containing a PLA-based amphiphilic copolymer bearing N-succinimidyl esters that can spontaneously react with a peptide/protein located in the aqueous phase. The relevancy of this strategy is supported by an improved antigenicity of immobilized HIV-1 Gag p24 protein.

Nanoprecipitation is considered as one of the most popular techniques to achieve biodegradable and biocompatible polylactide (PLA) based nanoparticles (NPs) for drug/vaccine delivery.^{1,2} Its advantages relies on the simplicity of the process (i.e., adding a water-miscible organic solution of the PLA/drug in water non-solvent, followed by removal of the organic solvent), which can be performed either with or without surfactants, as well as on the absence of emulsification phase, which is energy- and time-consuming.² Surface functionalization of these NPs with appropriate biomolecules is known to be a key issue regarding carrier efficiency. In drug delivery, coupling of cell targeting ligands (peptides, sugars) on NPs surface has shown to greatly enhance the selective delivery of the carrier in desired tissues or cells while preserving the safe ones.³⁻⁵ As for vaccine delivery, coupling of protein antigens and/or immunostimulatory molecules (such as ligands of antigen presenting cells) on NPs are found to induce enhanced adjuvant effect and immune responses.^{6,7} Generally, the biomolecules are introduced at the chain-end of PLA-b-poly(ethylene glycol) (PEG) or other PEG-based (Pluronic) amphiphilic block copolymers used as a surfactant in the PLA nanoprecipitation process, through two possible strategies: (i) the most used relies on biomolecule coupling after formation of the NPs through reaction of appropriately end-

functionalized PEG chain of the amphiphilic compound present at the NP surface (post-functionalization)^{4,8-11} or (ii) the amphiphilic PEG-based compound is first functionalized with the biomolecule and the obtained conjugate is involved in the nanoprecipitation process, leading to the functionalized NPs (pre-functionalization).¹²⁻¹⁴ The limitations of these approaches are, in the first case, a poor coupling yield due to reactions occurring in a heterogeneous phase and, in the second one, a possible unsuitable presentation of the biomolecule at the surface of the NPs. Moreover, whatever the above-mentioned approach, functionalization of PEGylated PLA NPs with biomolecules is tedious, generally requiring several steps for chemical derivatization of PEG chain end of the surfactants and further reaction with biomolecules. The search for more efficient and straightforward approaches to achieve functionalized NPs is thus becoming an urgent necessity to make the NP-based targeted drug/vaccine delivery strategy really attractive in the future. In recent studies, we reported an amphiphilic diblock copolymer composed of a PLA hydrophobic block, and a hydrophilic block bearing *N*-vinylpyrrolidone (NVP) and *N*-acryloxysuccinimide (NAS) units, through simple combination of ring-opening and nitroxide-mediated polymerizations.^{15,16} While NVP units impart stealthy character, similar to PEG,¹⁷ the pendant activated *N*-succinimidyl (NS) ester functions of the NAS units can be easily involved in coupling reactions with amino-bearing peptides and proteins without the need for any coupling agent.¹⁸ We took profit from this versatile NS ester based amphiphilic copolymer (i.e. PLA-b-P(NAS-co-NVP), referred as PLA-NS) to envision, for the first time, a one-step process, termed “reactive nanoprecipitation”, that allows simultaneously the formation of NPs and biomolecule coupling. Our strategy relies on the use of this copolymer as a surfactant with the PLA homopolymer and the drug in the water-miscible organic phase, while biomolecules (peptide, protein) are dissolved in the external aqueous phase buffered at a suitable pH (Figure 1). Upon addition of the polymer organic solvent in the non-solvent aqueous phase and formation of the NPs (as a result of diffusion of the organic solvent in water), the copolymer surfactant spontaneously anchors at the NP interface. As such, the pendant NS ester functions of the hydrophilic block become available for coupling of

^a Université Lyon 1, CNRS, LBTI UMR 5305, 7 Passage du Vercors, 69367 Lyon Cedex 07, France.

^b Aix-Marseille Université, CNRS, ICR UMR 7273, Avenue Escadrille Normandie Niemen, 13397 Marseille Cedex 20, France.

† Electronic Supplementary Information (ESI) available: Experimental details, supplementary tables and figures. See DOI: 10.1039/x0xx00000x

COMMUNICATION

the amino-bearing molecules, allowing functionalization of the NPs during the nanoprecipitation process.

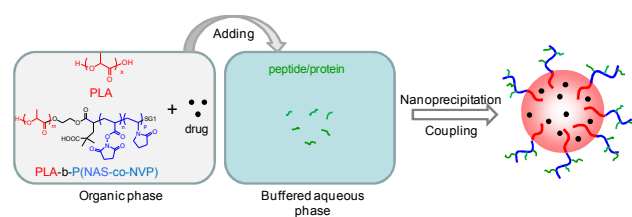


Fig. 1 Schematic view of “reactive nanoprecipitation” process leading to functionalized PLA NPs in one-step.

As a proof of concept, our strategy was first applied to a peptide, namely the KKKVQGEESNDK sequence derived from Interleukin 1 β (referred as ILP). The peptide was dissolved at various concentrations (0 to 0.48 mg mL⁻¹) in a 20 mM phosphate buffer at a pH of 8. The copolymer and homo-PLA (typically, 4 mg copolymer and 40 mg PLA) were dissolved in acetonitrile (4.4 mL, i.e. a total polymer concentration of 10 mg/mL). After formation of the NPs through the addition of this polymer organic phase in the peptide aqueous phase (1 vol. to 1 vol.), the non-coupled peptide and N-hydroxysuccinimide (NHS) produced upon coupling reaction were quantified in the supernatant by HPLC, as previously described.¹⁶ As shown in Figure 2a, the immobilized amount of peptide on NPs reached a plateau value close to 25 mg/g of NP. NHS peak area increased with increasing peptide amounts, indicating the covalent character of the immobilization (Figure 2a). An increase in zeta potential of the NPs was also observed with increasing peptide amounts, indicating the influence of the lysine amine cationic groups of the peptide at the NP surface (Figure 2b). The mean diameter of the NPs, determined by dynamic light scattering (DLS), was 320 nm, with a polydispersity index (PI) of 0.13 indicating a homogeneous size distribution. As a comparison, the NPs produced in the same conditions but in the absence of the peptide showed a mean diameter of 195 nm with a PI of 0.11. This increase in size showed the impact of the presence of the peptide in the aqueous phase during the nanoprecipitation process. This increase was particularly attributed to the more pronounced deployment of the NVP-NS based block corona during the process, favored by the coupling of the peptide, as result of increased hydrophilicity. SEM observation of the NPs in the presence or absence of the peptide supported the difference in size measured by DLS (Figures 3a and 3b, respectively). Finally, encapsulation of hydrophobic Nile Red probe as a model drug was performed during the one-step process, by dissolving the molecule in the acetonitrile organic phase along with the copolymer and the homo-PLA. The encapsulated Nile Red had no impact on the peptide coupling amounts and NP size and zeta potential (Table S1 and Figure S1, Supporting information section).

Journal Name

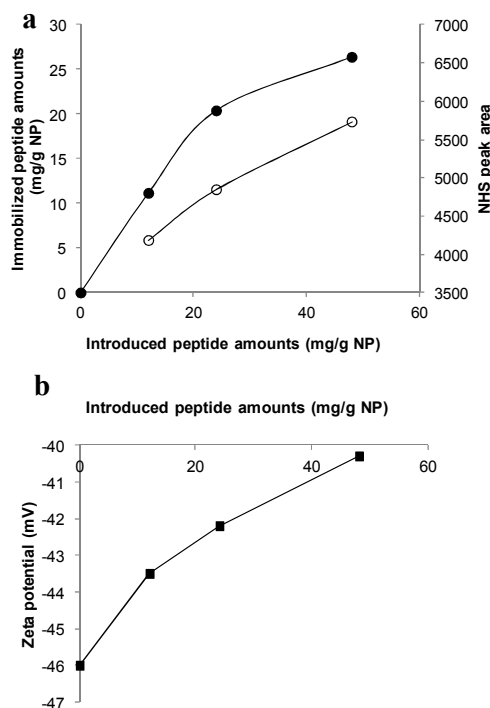


Fig. 2 (a) Immobilized ILP peptide amounts on NPs with corresponding NHS peak area in HPLC in the supernatant and (b) zeta potential of the NPs, as a function of introduced peptide amounts.

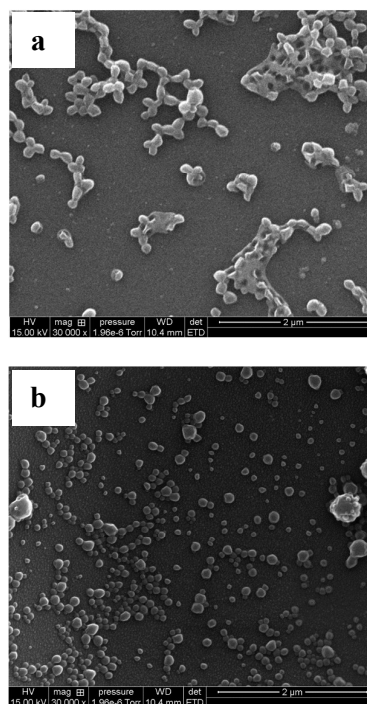


Fig. 3 SEM images of (a) peptide-functionalized and (b) non-functionalized NPs.

The “reactive nanoprecipitation” process was further evaluated for the preparation of protein antigen-functionalized NPs, using the HIV-1 Gag p24 model antigen, in a vaccine delivery perspective. To minimize protein denaturation that is known to possibly occur in the presence of organic solvents,^{19,20} an organic phase/aqueous phase volume ratio of 1/19 was used. The p24 protein was dissolved at 0.316 mg.mL^{-1} in PBS at a pH of 7.4, and the copolymer PLA-NS at 52.7 mg.mL^{-1} in DMSO (homo-PLA was not used here). Upon addition of the organic phase in the PBS phase in the above-mentioned ratio (i.e. final p24 and PLA-NS concentrations of 0.3 and 2.635 mg.mL^{-1} , respectively), micellar NPs of 180 nm in mean diameter ($PI = 0.25$) were formed. The immobilization of the p24 on the NPs was attested by SDS-polyacrylamide gel electrophoresis (PAGE) analysis, and was found to be nearly quantitative, since almost no free p24 was detected (lane 3, Figure S2, Supporting information section, vs. lane 2 for free p24 at the same concentration). The p24 functionalized NPs could be observed close to the start (lane 3, Figure S2), as a result of their incapacity, due to their size, to diffuse through the gel, as previously reported.²¹ The covalent character of the coupling was further confirmed by the fluorescamine assay, revealing 85% decrease in p24 amine groups, as a result of amide formation following coupling. The NPs exhibited a zeta potential of -31 mV ; this still negative value being attributed to the slightly negatively charged p24 ($pI=5.9$) close to neutral pH. The antigenicity of the so immobilized p24 was finally assessed through enzyme-linked immunosorbent assay (ELISA), and compared to free p24 in the same conditions (Figure 4). The detection system relied on the use of a biotinylated rabbit anti-p24 polyclonal antibody (Ab), followed by addition of horseradish peroxidase (HRP) conjugated streptavidin, and HRP-catalyzed reaction with 3,3',5,5'-tetramethylbenzidine (TMB) substrate with further quenching with sulfuric acid, for final absorbance measurement at 450 nm (see Supporting Information for details). The immobilized p24 induced an improved affinity for anti-p24 antibodies as compared to the free analog, whatever the antibody dilution and p24 concentration used for coating (10 or $1 \mu\text{g.mL}^{-1}$), as shown in Figures 4a and 4b. Interestingly, these results thus not only indicated that the integrity of the p24 immobilized on NPs was preserved, but also particularly disclosed that surface immobilization of p24 antigen on the NPs made the antigen more highly accessible for antibody recognition (Figure 4c). In conclusion we developed here a straightforward and efficient process based on the nanoprecipitation technique, allowing simultaneously the formation and surface functionalization of NPs. The relevancy of our approach was supported by an efficient biological activity of surface coupled protein antigen, granting access to further use of such functionalized NPs in vaccine/drug delivery applications.

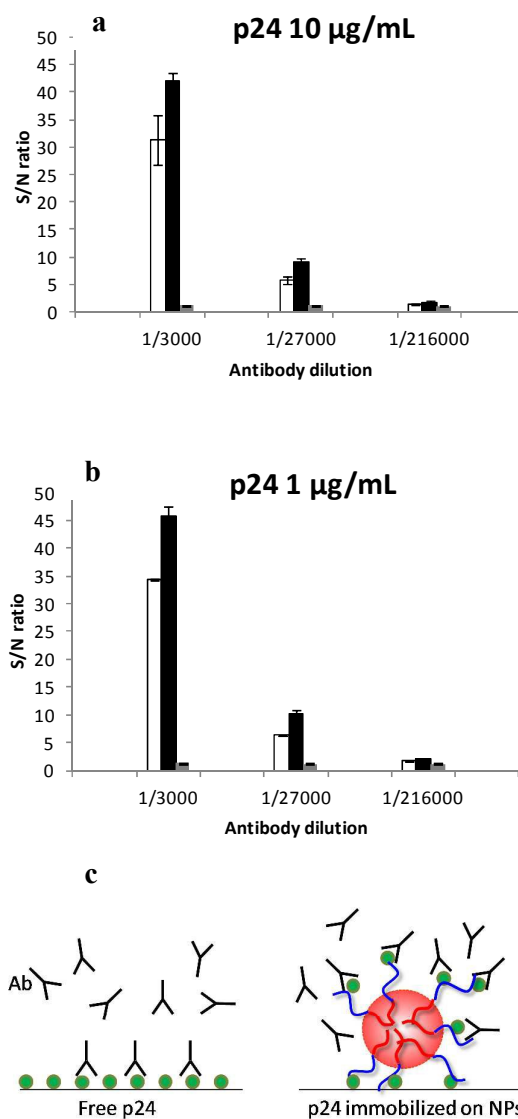


Fig. 4 Enzyme-linked immunosorbent assay (ELISA) of free (white) or immobilized (black) p24 (control NPs without p24 in grey). Coating of p24 (free or immobilized) was performed at $10 \mu\text{g.mL}^{-1}$ (a) or $1 \mu\text{g.mL}^{-1}$ (b). Signal to noise (S/N) ratio was the ratio of absorbance (450 nm) in the presence of Ab (at given dilution) to absorbance in absence of Ab; (c) schematic view of the improved Ab recognition through p24 immobilization on NPs, as evidenced by ELISA.

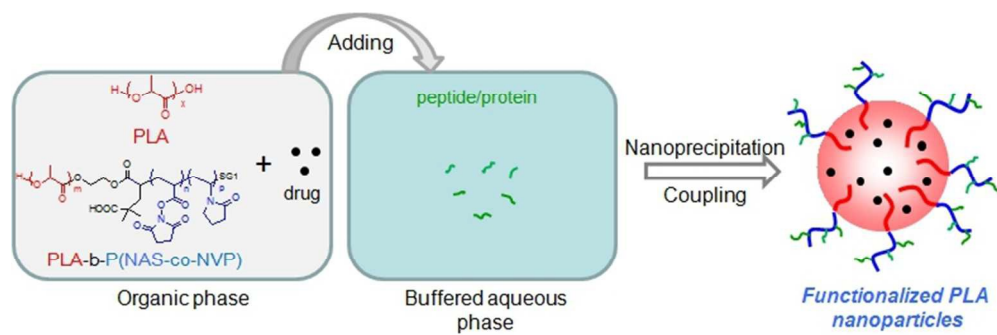
Acknowledgements

This work was funded by the ANR (French National Research Agency) through Euronanomed grant (iNanoDCs) and ANabio research projects, and Fondation Pierre Bergé (Sidaction) and Finovi to Bernard Verrier. This work was also partially supported by grants from the two FP7 European grants CUT'HIVAC (no 241904) and ADITEC (no 280873). The funders had no role in the study design,

data collection and analysis, decision to publish, or preparation of the manuscript.

References

- 1 H. Fessi, J.P. Devissaguet, F. Puisieux and C. Thies, *US Pat.*, 5118528, 1988.
- 2 S. Schubert, J. T. Delaney Jr, U. S. Schubert, *Soft Matter*, 2011, **7**, 1581-1588.
- 3 N. Kamaly, Z. Xiao, P. M. Valencia, A. F. Radovic-Moreno and O. C. Farokhzad, *Chem. Soc. Rev.*, 2012, **41**, 2971.
- 4 M. Prabaharan, J. J. Grailler, S. Pilla, D. A. Steeber and S. Gong, *Biomaterials*, 2009, **30**, 3009.
- 5 J. Cheng, B. A. Teply, I. Sherifia, J. Sunga, G. Luthera, F. X. Gua, E. Levy-Nissenbaum, A. F. Radovic-Moreno, R. Langer and O. C. Farokhzad, *Biomaterials*, 2007, **28**, 869.
- 6 A. des Rieux, V. Pourcelle, P. D. Cani, J. Marchand-Brynaert and V. Pr eat, *Adv. Drug Deliv. Rev.*, 2013, **65**, 833.
- 7 M. Garinot, V. Fi vez, V. Pourcelle, F. Stoffelbach, A. des Rieux, L. Plapied, I. Theate, H. Freichels, C. J r ome, J. Marchand-Brynaert, Y. J. Schneider and V. Pr eat, *J. Control. Release*, 2007, **120**, 195.
- 8 N. Nasongkla, X. Shuai, H. Ai, B. D. Weinberg, J. Pink, D. A. Boothman and J. Gao, *Angew. Chem.*, 2004, **116**, 6483.
- 9 N. Zhang, C. Chittapuso, C. Duangrat, T. J. Siahaan and C. Berkland, *Bioconjugate Chem.* 2008, **19**, 145.
- 10 A. Fakhari, A. Baoum, T. J. Siahaan, K. B. Le and C. Berkland, *J. Pharm. Sci.*, 2011, **100**, 1045.
- 11 D. H. Yu, Q. Lu, J. Xie, C. Fang and H. Z. Chen, *Biomaterials*, 2010, **31**, 2278.
- 12 P. M. Valencia, M. H. Hanewich-Hollatz, W. Gao, F. Karim, R. Langer, R. Karnik and O.C. Farokhzad, *Biomaterials*, 2011, **32**, 6226.
- 13 Y. B. Patil, U. S. Toti, A. Khair, L. Ma and J. Panyam, *Biomaterials*, 2009, **30**, 859.
- 14 V. Fievez, L. Plapied, A. des Rieux, V. Pourcelle, H. Freichels, V. Wascotte, M.L. Vanderhaeghen, C. J r ome, A. Vanderplasschen, J. Marchand-Brynaert, Y. J. Schneider and V. Pr eat, *Eur. J. Pharm. Biopharm.*, 2009, **73**, 16.
- 15 N. Handk , T. Trimaille, E. Luciani, M. Rollet, T. Delair, B. Verrier, D. Bertin and D. Gigmes, *J. Polym. Sci. A Polym. Chem.* 2011, **49**, 1341.
- 16 N. Handk , D. Ficheux, M. Rollet, T. Delair, K. Mabrouk, D. Bertin, D. Gigmes, B. Verrier and T. Trimaille, *Colloids Surf. B*, 2013, **103**, 298.
- 17 K. Knop, R. Hoogenboom, D. Fischer and U. S. Schubert, *Angew. Chem. Int. Ed.*, 2010, **49**, 6288.
- 18 A. Das and P. Theato, *Chem. Rev.* 2015, DOI: 10.1021/acs.chemrev.5b00291.
- 19 K. Griebenow and A. M. Klibanov, *J. Am. Chem. Soc.*, 1996, **118**, 11695.
- 20 Y. L. Khmelnitsky, V. V. Mozhaev, A. B. Belova, M. V. Sergeeva and K. Martinek, *Eur. J. Biochem.*, 1991, **198**, 31.
- 21 M. J. Heffernan and N. Murthy, *Ann. Biomed. Eng.*, 2009, **37**, 1993.



279x92mm (72 x 72 DPI)